Science & Technology Development Journal 2023, 26(4):3035-3047

Open Access Full Text Article

Original Research

Design and modeling of the nonlinear properties of octagonal lattice $Ge_{20}Sb_5Se_{75}$ photonic crystal fibers

Nguyen Thi Thuy*

ABSTRACT

Most silica photonic crystal fibers have limited spectral broadening in the infrared region, making them less than ideal in terms of technological applications. In this work, we propose a new $Ge_{20}Sb_5Se_{75}$ chalcogenide octagonal photonic crystal fiber that provides diverse dispersions with all-normal and anomalous regimes and multiple zero-dispersion wavelengths. The nonlinear properties are investigated over a wide wavelength range up to 14 μm by numerically solving Maxwell's wave equations using Lumerical Mode Solutions software. The full-vector finite-difference eigenmode method minimizes the losses so that low confinement losses in the short-wavelength region of $1 - 6$ μm are found and nonlinear coefficients as high as thousands of $W^{-1}.km^{-1}$ are achieved. Three fibers with an all-normal dispersion profile and anomalous dispersion with one or three zero dispersion wavelengths are proposed for supercontinuum generation. The fibers provide small dispersion values of −0.88, 0.08, and 1.646 ps/(nm.km) at suitable pump wavelengths. Furthermore, the very small confinement loss of approximately 10^{-5} to 10^{-11} dB/m is the outstanding advantage of these optical fibers. A broadband spectrum with low input power is expected as a result of the proposed fiber-based supercontinuum generation.

Key words: Ge20Sb5Se75 photonic crystal fibers, octagonal lattice, small dispersion, high nonlinear coefficient, low confinement loss

University of Education, Hue University, 34 Le Loi, Hue City, Viet Nam

Correspondence

Nguyen Thi Thuy, University of Education, Hue University, 34 Le Loi, Hue City, Viet Nam

Email: nguyenthithuy@dhsphue.edu.vn; ntthuy@hueuni.edu.vn

History

- Received: 2023-10-15
- Accepted: 2023-12-26
- Published Online: 2023-12-31

DOI :

https://doi.org/10.32508/stdj.v26i4.4200

INTRODUCTION

Broadening the output pulse in the mid-infrared (MIR) and infrared (IR) spectral regions is difficult when silica photonic crystal fibers (PCFs) are used for supercontinuum (SC) generation due to the high material absorption of glass. This is also the main limitation of silica PCFs, although this material is very popular and very easy to spin. To overcome this problem, many solutions, such as silica PCFs with various geometries[1,2] or liquid infiltration into hollow cores[3,4], have been demonstrated to further improve their SC generation performance. However, the application of these PCFs in wide wavelength ranges (MIR, IR) is still a major challenge for research groups. In recent years, chalcogenide (ChG) glasses have become known as excellent nonlinear materials with the ability to provide SC spectra in a wavelength range as wide as 20 μm[5,6]. Compared with silica, ChG glasses have higher optical transparency, higher linear and nonlinear refractive indices, lower phonon energy and greater optical transparency[7]. These compounds are formed mainly by chalcogenized elements of group XVI (S, Se and Te) and covalently bonded to Ge, As and Sb of group XV or Ge and Si of group XIV. Along with the flexibility in the structural design of PCFs, these beneficial properties are exploited and demonstrated numerically or experimentally for generating very broad bandwidths and highly coherent SC sources.

By numerical simulation, work[8] reported that As_2Se_3 hexagonal PCFs can produce low dispersion values of 19.92, 8.19, 4.06, and 15 ps. (nm/km) at pump wavelengths of 2.05, 3.1, 3.5, and 4.0 μm, respectively, with variations in the lattice constant Λ and the filling factor d/Λ (Λ = 1.0 μm, d/Λ = 0.8; Λ = 2.5 μm, d/Λ = 0.6; Λ = 3.0 μm, d/Λ = 0.5; and Λ = 3.5 μm, d/Λ = 0.5). These PCFs enabled SC with a spectrum extension from 2 to 15 μm. Article[9] numerically proved that a $Ge_{15}Sb_{15}Se_{70}$ circular lattice-PCF has an all-normal dispersion profile with a small effective mode area and high Kerr nonlinearity up to 1.96 $W^{-1}.m^{-1}$ at 3 μm, but the investigated wavelength area is only up to 8 μm. The effective mode area and nonlinear coefficient of $Ga_8Sb_{32}S_{60}$-PCF (Λ = 2.5 μm, d/Λ = 0.352) with a hexagonal structure of[10] are 15.23 μm^2 and 970 $W^{-1}.km^{-1}$ at 4.5 μm, respectively, as verified by simulations of ultraflat MIR SC generation. A $Ga_8Sb_{32}S_{60}$-PCF with a length of 9 mm and rectangular core was demonstrated to generate SC spectra with a MIR broadband due to its small all-normal dispersion. The values change from −19.52 ps/(nm.km) to

Cite this article : Thuy N T. **Design and modeling of the nonlinear properties of octagonal lattice $Ge_{20}Sb_5Se_{75}$ photonic crystal fibers**. *Sci. Tech. Dev. J.* 2023; 26(4):3035-3047.

−11.78 ps/(nm.km) at a pump wavelength of 4.0 μm as diameter d_1 increases from 1.3 to 1.9 μm with Λ = 2.5 μm [11]. Adjusting the diameter d of the air holes in the hexagonal cladding of $As_{39}Se_{61}$-PCF dominated the dispersion properties in favor of SC generation in the MIR region. Additionally, a PCF with Λ = 2.5 μm and d = 0.7 μm was reported to have a small effective mode area and a high nonlinear coefficient at 3.45 μm, which are 6.8 μm^2 and 5.89 $W^{-1}.m^{-1}$, respectively [12]. The generation of SCs in the MIR region with high coherence was reported in [13] based on $GeSe_2$-As_2Se_3-PbSe-PCFs with optimized dispersion. A dispersion value of −100 ps/(nm.km) at 3.1 μm was found for the structure Λ = 2.5 μm, d = 1.3 μm, but the nonlinearity was not as high as approximately 100 $W^{-1}km^{-1}$ with d = 0.65. Reference [14] also numerically analyzed the possibility of enabling MIR ultrabroadband SC generation based on a $Ge_{11.5}As_{24}Se_{64.5}$-circular PCF with a low dispersion value. The variation in the lattice constant Λ_1 leads to a variation in the dispersion, the value of which varies from −2.62 ps/(nm.km) at Λ_1 = 1.68 μm to −0.69 ps/(nm.km) at Λ_1 = 1.75 μm. Furthermore, the effective mode area also changes from 5.66 μm^2 to 5.30 μm^2 when Λ_1 is adjusted from 1.75 to 1.70 μm.

In the present study, ChG-PCFs were fabricated quite conveniently using stack-and-draw methods, and the mid-infrared SC generation spans ∼2.0 to 15.1 μm in 3 cm long As_2Se_3 and $AsSe_2$ fibers. Additionally, $Ge_{15}Sb_{20}Se_{65}$-PCFs spun into bare glass fibers have a loss of approximately 1.68 dB/m at 6.0 μm according to the melt-quenching method; these fibers are good candidates for highly sensitive temperature sensors [15,16]. Different methods, such as the casting method [17], combined extrusion method [18], and rod-in-tube drawing technique [19], have been shown to improve and enhance the quality of ChG-based SC generation-PCFs.

Obviously, ChG-PCF, as an interesting nonlinear medium for SC generation in the IR and MIR regions, has been verified through previous publications. The variations in the geometry of the lattice, the arrangement of the air holes in the cladding, and even the variety in the shape design of the core strongly influence the improvement in the dispersion and nonlinear properties of the fibers. Lattice types with high symmetry, such as hexagonal, circular, rectangular, and suspended cores, are preferred for design, but changing many lattice parameters at the same time can lead to complex fiber manufacturing. There are very few papers mentioning octagonal ChG-PCFs, and publication [20] showed the ability to improve the dispersion of octagonal As_2Se_3-PCFs. The values of characteristic quantities such as dispersion, nonlinear coefficient, and effective mode area are 77.55 ps/(nm.km), 4506 $W^{-1}.km^{-1}$, and 6 μm^2, respectively, at 1.55 μm, which is suitable for SC generation. The dispersion properties and nonlinear properties of $Ge_{20}Sb_5Se_{75}$-PCFs over a broad wavelength range up to 14 μm are investigated in numerical detail and reported in this work. The same air holes are arranged evenly in the cladding in an octagonal fashion. A flat dispersion with a very small value of approximately 1.0 ps/(nm.km) and high nonlinearity coefficients of thousands of $W^{-1}.km^{-1}$ are achieved. Interestingly, very low confinement losses, as low as approximately 10^{-11} dB/m at a suitable pump wavelength, were obtained. This makes the proposed optimal PCFs quite necessary for broadband SC generation in the MIR region with low peak power.

MATERIALS-METHODS

Lumerical Mode Solutions software assisted us in designing the structures of the $Ge_{20}Sb_5Se_{75}$-PCFs. First, the $Ge_{20}Sb_5Se_{75}$ material is introduced into the data system by determining the Sellmeier coefficient of the linear refractive index according to **Equation (1)** [21]. Second, we build a subroutine for the octagonal structure. There are eight layers of air holes with diameter $d = (0.3 - 0.75)\Lambda$, with Λ being the distance between two adjacent holes (lattice constant) surrounding a core with diameter $Dc = 2\Lambda - d$. The values of Λ are 2.2, 2.5, 4.5, and 5.0 μm. The position of the air holes is calculated so that they are evenly spaced and parallel to the axis of the core and then attached to the system. Finally, we chose the refractive indices of the air in the available data to determine the entrance into the holes in the cladding. The shape of the PCF in two dimensions is illustrated in **Figure 1**a. The refractive index of the $Ge_{20}Sb_5Se_{75}$ material was extrapolated according to [21] and is shown in **Figure 1**b. The values decrease with increasing wavelength, but the decrease in the refractive index is faster in the short-wavelength region from 1 to 2 μm.

$$n(\lambda) = \sqrt{1 + \frac{4.761\lambda^2}{\lambda^2 - 0.0356} + \frac{0.06994\lambda^2}{\lambda^2 - 0.6364} + \frac{0.893\lambda^2}{\lambda^2 - 491.72}} \quad (1)$$

where λ is the wavelength and $n(\lambda)$ is the refractive index of the material.

The propagation of electromagnetic modes in nonlinear media such as $Ge_{20}Sb_5Se_{75}$-PCFs is modeled by solving Maxwell's wave equations. The cross-section of the fibers is divided into a very large number of very small rectangles to minimize losses using the

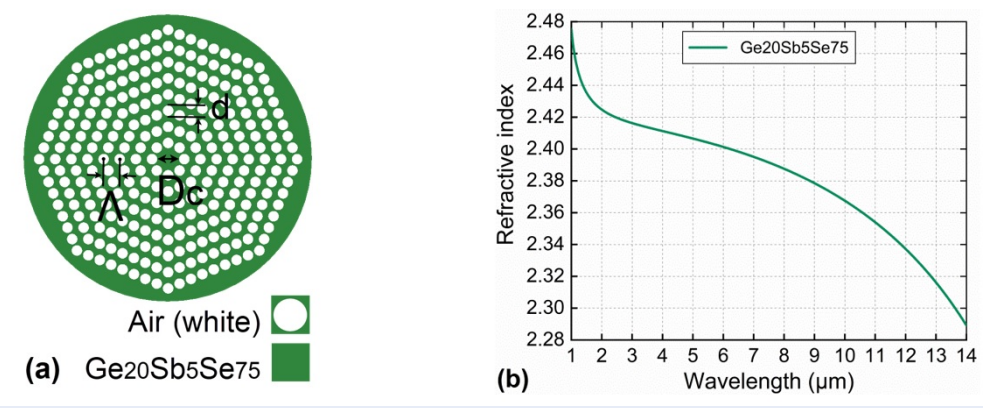

Figure 1: The shape of $Ge_{20}Sb_5Se_{75}$-PCF in two-dimensional space with the core in the center and eight surrounding layers of air holes. The white represents air filling into the holes and the green represents the $Ge_{20}Sb_5Se_{75}$ base material (**a**). The decrease of linear refractive index with respect to wavelength is extrapolated according to [21] (**b**).

full-vector finite-difference eigenmode method. Furthermore, the boundary condition is chosen to be perfectly matched layers to help maximize light absorption and minimize reflection at the boundary. The good light confinement in the core of $Ge_{20}Sb_5Se_{75}$-PCFs is illustrated in **Figure 2**.

Dispersion is a typical phenomenon of optical fibers and is characterized by how fast the pulse's different frequency components move due to interactions with the electrons of the medium, described by **Equation (2)**[22]. PCFs with suitable dispersion properties, such as flatness over a wide wavelength range, small gradients, and low values at pump wavelengths, are always important factors in improving the quality of the SC process.

$$D(\lambda) = -\frac{\lambda}{c}\frac{d^2 Re\left[n_{eff}\right]}{d\lambda^2} \quad (2)$$

where $\mathrm{Re}[n_{eff}]$, λ, and c are the real parts of the effective refractive index, the wavelength, and the speed of light in a vacuum, respectively.

When the laser pulse propagates in an optical fiber, the quantity responsible for the dispersive temporal broadening of pulses is expressed in the group velocity dispersion (GVD) parameter (β_2) as follows[20]:

$$\beta_2 = -\frac{\lambda D(\lambda)}{2\pi c} \quad (3)$$

Further SC spectral broadening at the edges depends on the nonlinear characteristics of PCFs, such as confinement loss (L_c), the nonlinear coefficient (γ), and the effective mode area (A_{eff}), which are determined through the following formula[22]:

$$L_c = 8.686\frac{2\pi}{\lambda} Im\left[n_{eff}\right] \quad (4)$$

where Im $[n_{eff}]$ is the imaginary part of the effective refractive index. The confinement loss is one of the characteristic quantities of PCFs; it represents the degree to which information is confined in the core and is not scattered when the laser pulse is transmitted. Structural parameters such as the air hole diameter and lattice constant affect the confinement loss.

$$\gamma(\lambda) = 2\pi\frac{n_2}{\lambda A_{eff}} \quad (5)$$

where n_2 is the nonlinear refractive index of $Ge_{20}Sb_5Se_{75}$. The nonlinear coefficient quantifies the strength of the nonlinear interaction relative to the Kerr nonlinearity of the medium. PCFs with higher nonlinearities are more beneficial for low-peak power SC sources. The nonlinear coefficient quantifies the strength of the nonlinear interaction relative to the Kerr nonlinearity of the medium. PCFs with higher nonlinearities are more beneficial for low-peak power SC sources. The nonlinear coefficient is inversely proportional to the effective mode area, which represents the area that the wave guide or fiber mode effectively covers in terms of transverse dimensions.

$$A_{eff} = \frac{\left(\int_{-\infty}^{\infty}\int_{-\infty}^{\infty}|E|^2 dxdy\right)^2}{\int_{-\infty}^{\infty}\int_{-\infty}^{\infty}|E|^4 dxdy} \quad (6)$$

RESULTS

Normal and anomalous dispersion is achieved in optical fibers due to the increase or decrease in the refractive index with increasing wavelength. Typically, a normal dispersion is observed as the refractive index decreases with increasing wavelength. However, in small wavelength ranges, the absorption of radiation

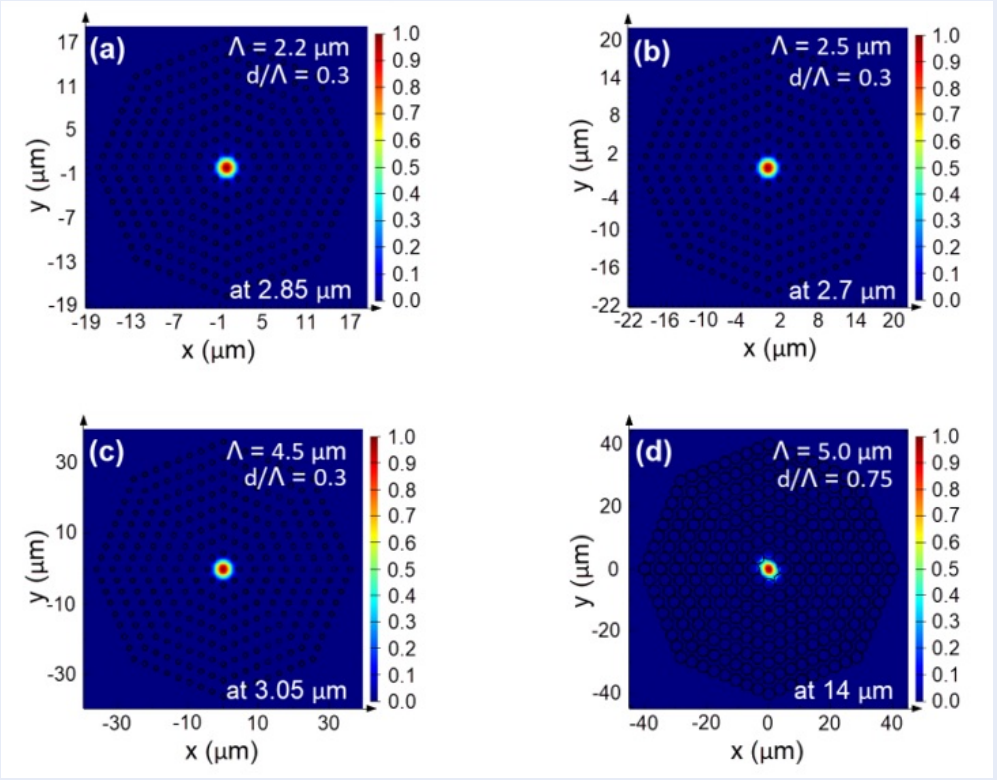

Figure 2: The images illustrate the confinement of light in the core of $Ge_{20}Sb_5Se_{75}$-PCFs.

causes the refractive index to increase with increasing wavelength, a phenomenon known as anomalous dispersion.

$Ge_{20}Sb_5Se_{75}$-PCFs have diverse dispersion properties over a wide wavelength range, as shown in **Figure 3**. Most anomalous dispersions with one, two or even three zero dispersion wavelengths (ZDWs) are found. There is only one all-normal dispersion for a PCF with structure $\Lambda = 2.2$ μm and $d/\Lambda = 0.3$. For small PCFs ($\Lambda = 2.2$ and 2.5 μm), the majority of the dispersion curves have a typical parabolic profile, separating normal and anomalous dispersion regions in the investigated wavelength range. When $\Lambda = 2.2$ μm, except for the only all-normal dispersion curve, the remaining structures all have anomalous dispersion with two ZDWs in the wavelength range up to 8 μm. For PCFs with $\Lambda = 2.5$ μm, we obtain two dispersion curves with three ZDWs corresponding to the structures $\Lambda = 2.5$ μm, $d/\Lambda = 0.3$ and $\Lambda = 2.5$ μm, $d/\Lambda = 0.35$. When the size of the PCFs is further increased ($\Lambda = 4.5$ and 5.0 μm), only anomalous dispersion curves are observed with one ZDW. Furthermore, the dispersion curves tend to shift above the zero dispersion curve as d/Λ increases from 0.3 to 0.75. Therefore, ZDW_{1s} increasingly shift toward shorter wavelengths, while ZDW_{2s} and ZDW_{3s} shift toward longer wavelengths. **Table 1** shows the values of ZDWs when Λ and d/Λ vary. The ZDW_1 of PCFs with $\Lambda = 2.2$ and 2.5 μm has a value close to the wavelength of 1.55 μm, which is the wavelength of common commercial laser sources. This finding implies that we choose appropriate pump wavelengths for SC generation. However, some studies on ChG-PCFs[5,8,9] have verified that suitable pump wavelengths can be selected in the MIR or IR region. Due to the rapid development of fiber optic technology today, choosing a pump wavelength in any region is feasible in practice.

The relationships between the GVD parameter and wavelength and between the GVD parameter and the variation in the structural parameters are shown in **Figure 4**. In the wavelength region smaller than approximately 4 μm, the difference in GVD values of the structures is not large. At best, the separation between the curves is clearer in the longer wavelength region. The GVD will be either positive or negative depending on whether the fiber is a normal or anomalous dispersive type. The GVD increases rapidly in the wavelength region greater than 6 μm.

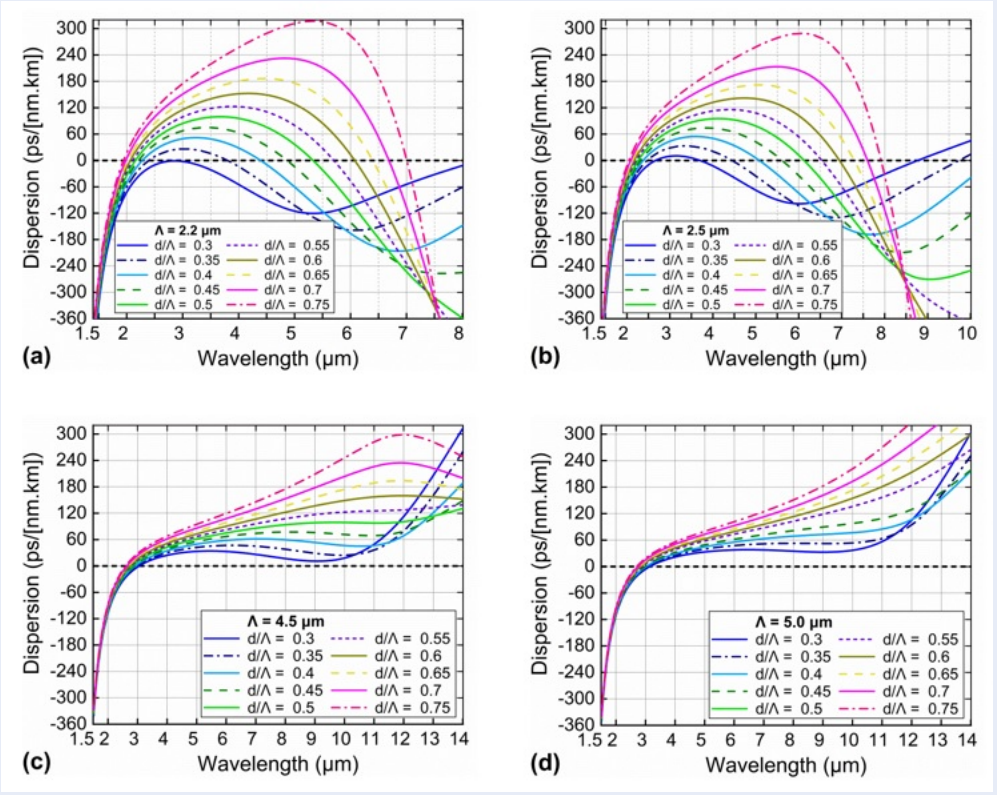

Figure 3: The all-normal and anomalous dispersions with multiple ZDWs of $Ge_{20}Sb_5Se_{75}$-PCFs when d/Λ varies from 0.3 to 0.75, with $\Lambda = 2.2\ \mu$m (**a**), 2.5 μm (**b**), 4.0 μm (**c**), and 5.0 μm (**d**).

Table 1: The ZDWs of $Ge_{20}Sb_5Se_{75}$-PCFs with variations in Λ and d/Λ

	$\Lambda = 2.2\ \mu$m		$\Lambda = 2.5\ \mu$m			$\Lambda = 4.5\ \mu$m	$\Lambda = 5.0\ \mu$m
d/Λ	ZDW_1	ZDW_2	ZDW_1	ZDW_2	ZDW_3	ZDW_1	ZDW_1
0.3	D < 0	D < 0	2.663	3.706	8.736	3.048	3.141
0.35	2.391	3.804	2.468	4.455	9.729	2.976	3.075
0.4	2.277	4.399	2.375	5.088		2.917	3.021
0.45	2.207	4.87	2.313	5.627		2.868	2.973
0.5	2.152	5.340	2.260	6.144		2.818	2.835
0.55	2.107	5.707	2.214	6.544		2.774	2.881
0.6	2.063	6.084	2.170	6.978		2.728	2.835
0.65	2.021	6.430	2.127	7.308		2.683	2.791
0.7	1.981	6.702	2.086	7.686		2.638	2.745
0.75	1.940	7.07	2.044	7.958		2.591	2.699

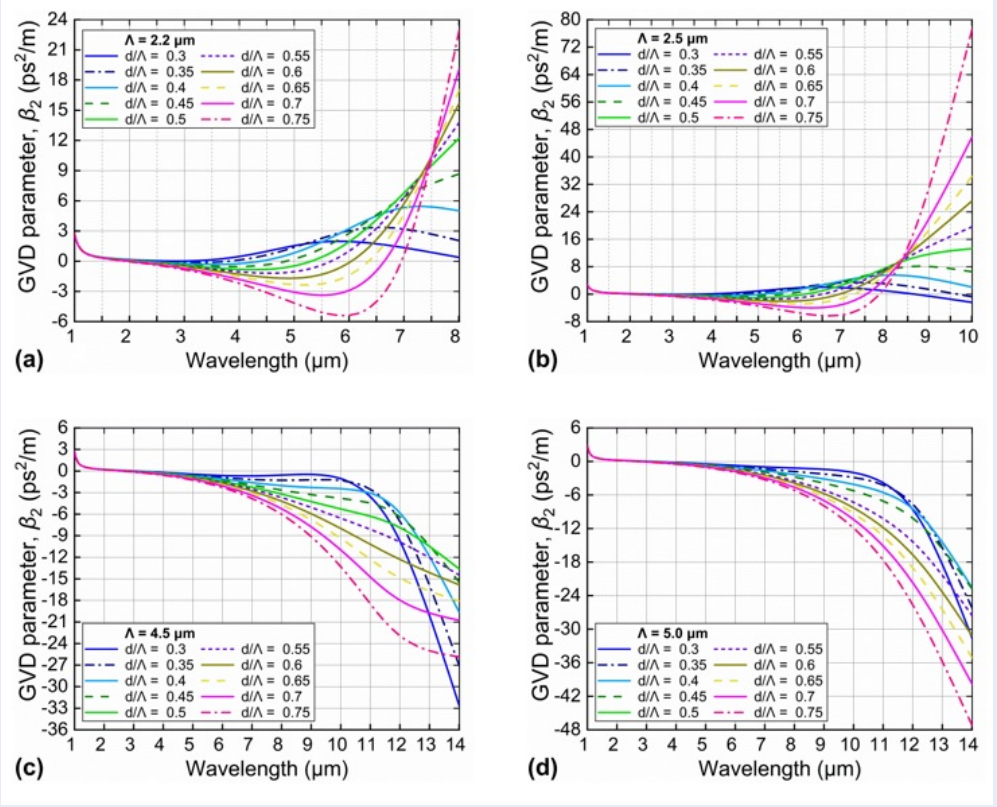

Figure 4: The graph of GVD against wavelength of $Ge_{20}Sb_5Se_{75}$-PCFs when d/Λ vary from 0.3 to 0.75, with Λ = 2.2 μm (**a**), 2.5 μm (**b**), 4.5 μm (**c**), and 5.0 μm (**d**).

Based on the preliminary dispersion and GVD parameter results, three optical fibers with suitable dispersion and GVD values are introduced to study in detail the characteristic quantities required for the SC process. The names of the fibers are #F_1, #F_2, and #F_3, with the structural parameters Λ = 2.2 μm, d/Λ = 0.3; Λ = 4.5 μm, d/Λ = 0.3; and Λ = 2.5 μm, d/Λ = 0.3. **Figure 5** – **Figure 9** displays the dispersion and quantities that characterize the nonlinear properties of the three fibers. The values of dispersion, GVD parameter, confinement loss, nonlinearity coefficient, and effective mode area at the pump wavelengths are calculated and indicated in **Table 2**.

DISCUSSION

Dispersion is a very important factor in choosing a suitable fiber for SC processes with all-normal or anomalous dispersion characteristics. In addition, the number of ZWWs in dispersion profiles governs the spectral characteristics related to soliton dynamics. Fiber #F_1 (Λ = 2.2 μm, d/Λ = 0.3) possesses all-normal dispersion and has a local maximum at a wavelength of approximately 2.8 μm (**Figure 5**). The expected pump wavelength for SC generation is 2.85 μm. A low dispersion value of −0.88 ps/(nm.km) was obtained at this wavelength (**Table 2**). Compared to previous publications on SCs based on ChG-PCFs with all-normal dispersion, the dispersion value achieved is approximately 13 times lower than [11], 113 times lower than [13], and 3 times lower than [14]. A low dispersion at a suitable pump wavelength is an ideal condition for enabling an SC with a boad spectrum and high coherence under the control of the self-phase modulation effect and optical wave breaking. This phenomenon occurs because the energy is transferred sequentially from high frequency to low frequency in the pulse by stimulated Raman scattering [23], leading to the suppression of soliton dynamics. The dispersion curve of fiber #F_2 (Λ = 4.5 μm, d/Λ = 0.3) is divided into two regimes: normal and anomalous dispersion (**Figure 5**), with ZDW = 3.048 μm. The recommended pump wavelength is 3.05 μm so that the fiber is pumped in an anomalous dispersion regime. Typically, the SC spectrum is much broader than that of a fiber pumped in the normal dispersion

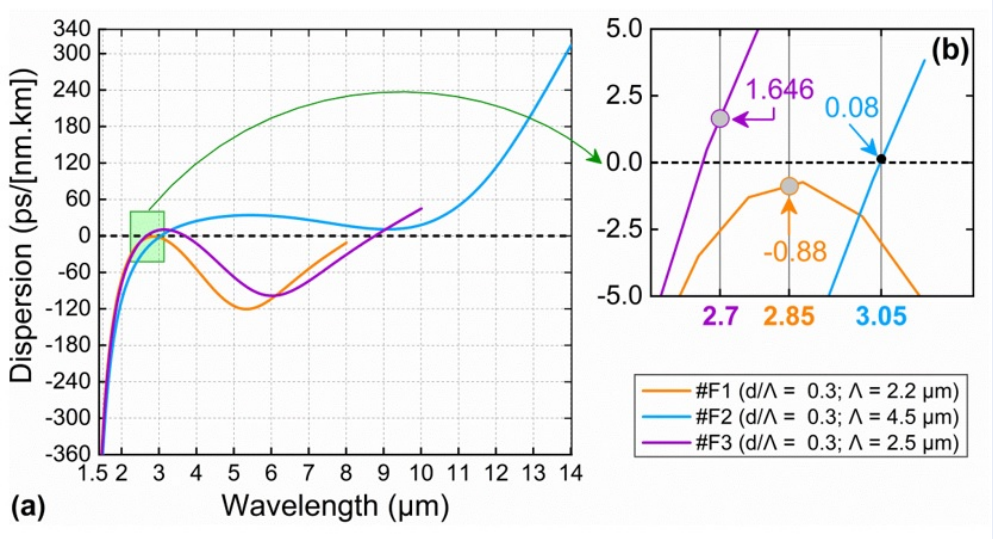

Figure 5: The dispersions curves with multiple ZDWs of proposed fibers, #F_1 (Λ = 2.2 μm, d/Λ = 0.3), #F_2 (Λ = 4.5 μm, d/Λ = 0.3), and #F_3 (Λ = 2.5 μm, d/Λ = 0.3) (**a**). The dispersion values of fibers at pump wavelengths (**b**).

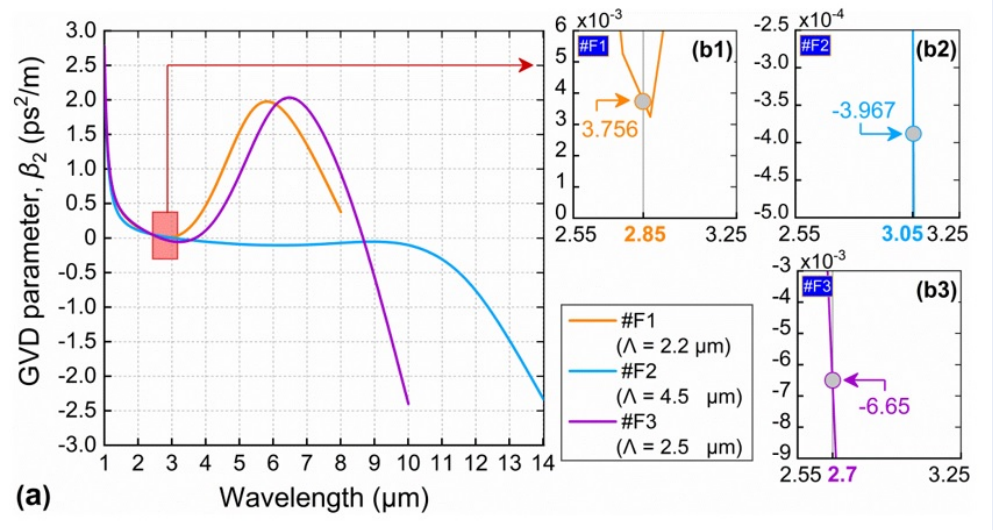

Figure 6: The dependence of GVD parameter on the wavelength of proposed fibers, #F_1 (Λ = 2.2 μm, d/Λ = 0.3), #F_2 (Λ = 4.5 μm, d/Λ = 0.3), and #F_3 (Λ = 2.5 μm, d/Λ = 0.3) (**a**). The GVD parameter values of fibers at pump wavelengths (**b**).

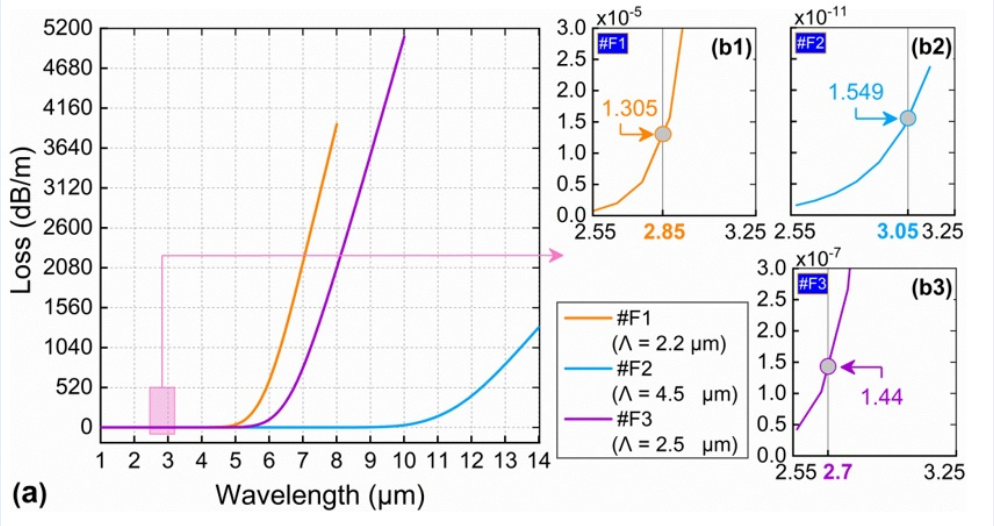

Figure 7: The dependence of confinement loss on the wavelength of proposed fibers, #F_1 ($\Lambda = 2.2\ \mu$m, $d/\Lambda = 0.3$), #F_2 ($\Lambda = 4.5\ \mu$m, $d/\Lambda = 0.3$), and #F_3 ($\Lambda = 2.5\ \mu$m, $d/\Lambda = 0.3$) (**a**). The confinement loss values of fibers at pump wavelengths (**b**).

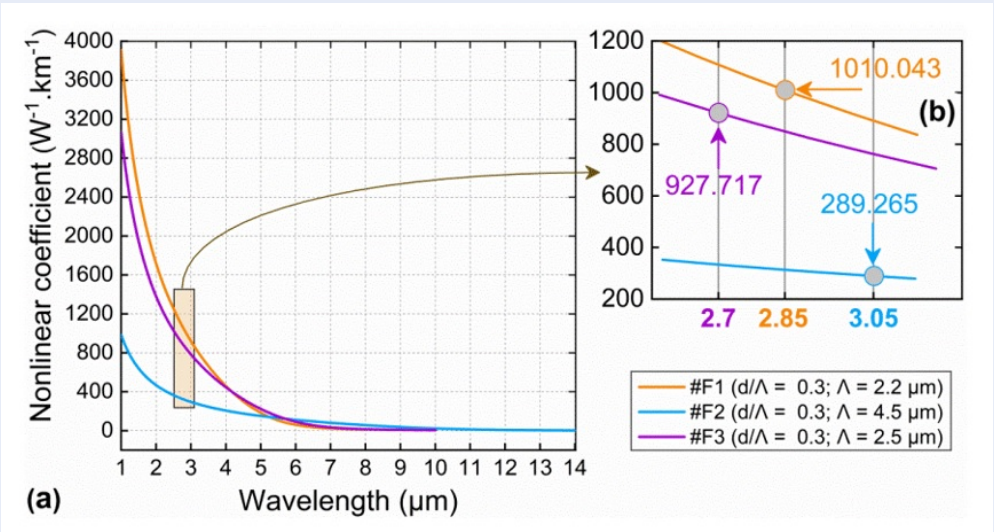

Figure 8: The dependence of nonlinear coefficient on the wavelength of proposed fibers, #F_1 ($\Lambda = 2.2\ \mu$m, $d/\Lambda = 0.3$), #F_2 ($\Lambda = 4.5\ \mu$m, $d/\Lambda = 0.3$), and #F_3 ($\Lambda = 2.5\ \mu$m, $d/\Lambda = 0.3$) (**a**). The nonlinear coefficient values of fibers at pump wavelengths (**b**).

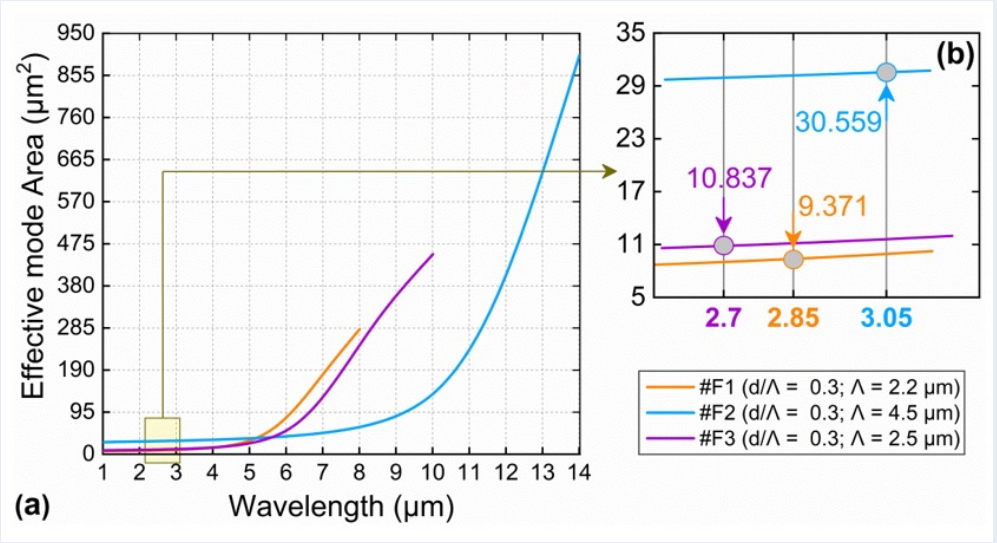

Figure 9: The effective mode area on the wavelength of proposed fibers, #F_1 ($\Lambda = 2.2\ \mu m$, $d/\Lambda = 0.3$), #F_2 ($\Lambda = 4.5\ \mu m$, $d/\Lambda = 0.3$), and #F_3 ($\Lambda = 2.5\ \mu m$, $d/\Lambda = 0.3$) (**a**). The effective mode area values of fibers at pump wavelengths (**b**).

Table 2: The structural parameters and the values of the characteristic quantities at the pump wavelength of the three proposed fibers

#	Dc	Λ	d/Λ	Pump wavelength	D	$\beta 2$	Lc	γ	A_{eff}
	μm	μm		μm	ps/nm.km	ps^2/m	dB/m	$W^{-1}.km^{-}$	μm^2
#F_1	3.74	2.2	0.3	2.85	−0.880	3.756	$1.305\times10^{-}$	1010.043	9.371
#F_2	7.65	4.5	0.3	3.05	0.080	−3.967	$1.549\times10^{-}$	289.265	30.559
#F_3	4.25	2.5	0.3	2.70	1.646	−6.650	$1.440\times10^{-}$	921.717	10.837

regime due to the impact of soliton effects such as soliton fission, self-shifting soliton frequency, and dispersion waves[23–25]. Moreover, with a very low dispersion value of 0.08 ps/(nm.km) at the pump wavelength (**Table 2**), this fiber is expected to generate a high-quality SC. Fiber #F_3 ($\Lambda = 2.5\ \mu m$, $d/\Lambda = 0.3$) has anomalous dispersion with three ZDWs, so the dispersion region is divided into four parts (**Figure 5**). With a dispersion value of 1.646 ps/(nm.km) at 2.7 μm, close to ZDW_1 (2.663 μm), the proposed fiber pumps are in the first anomalous dispersion regime, so soliton dynamics remain the main mechanism for broadening the SC spectrum. Furthermore, a soliton shift can occur from the first anomalous dispersion region to the second anomalous dispersion region, causing the spectrum to continue to broaden[26]. In addition, effects such as phase modulation and four-wave mixing are created on the left side of the ZDWs, causing a green shift in the trapped wave, which also helps increase the bandwidth[26]. The dispersion values obtained at the pump wavelength for fibers #F_1 and #F_2 are much lower than those in reference[8]. The GVD parameter is proportional to dispersion and characterizes the influence of the medium on the duration of an optical pulse. The GVD values at the pump wavelengths of the three proposed fibers are 3.756, −3.967, and −6.650 ps^2/m. Fiber #F_1 has the lowest dispersion value corresponding to the smallest GVD.

The confinement loss of fibers #F_1, #F_2, and #F_3 increases rapidly in the long-wavelength region ($\lambda > 5.0\ \mu m$) (**Figure 7**) due to the leakage of low-frequency components from the core to the cladding or between air holes. This also leads to a large effective mode area in this wavelength region. In addition, the nonlinear coefficient is also reduced because it is inversely proportional to the effective mode area. Therefore, all the

fibers had a pump wavelength chosen to be less than 5.0 μm. Among the three fibers, fiber #F_2 has the smallest L_c value (1.549×10^{-11} dB/m) and the lowest dispersion value compared to the others, but it has the largest effective mode area and smallest nonlinear coefficient (**Table 2**). This opens up the opportunity to create broadband SCs using #F_2 fibers. The larger the L_c is, the more the spectrum is limited to broadening at the red edge. It should be noted that it is difficult to simultaneously optimize the nonlinear characteristics of the fibers because the fibers are advantageous because they can be used to generate appropriate SC orientations. Fiber #F_1 has the smallest effective mode area, leading to the highest nonlinear coefficient, and the dispersion value of −0.88 ps/(nm.km) is smaller than that of fiber #F_3. Although the L_c of this fiber is the largest among the three fibers, it is still quite small compared to that in some previous publications[5,8]. This fiber can be used as a broad-spectrum and low-peak-power SC source due to the high nonlinearity at the pump wavelength. Fiber #F_3 is still expected to produce a broadband SC under the influence of soliton dynamics, although this approach does not have outstanding advantages when considering the value of nonlinear characteristic quantities. A rather small L_c value of 1.440×10^{-7} dB/m and a rather high nonlinearity coefficient of 921.717 $W^{-1}.km^{-1}$ at a pump wavelength of 2.7 μm are necessary conditions for obtaining a broad-spectrum SC with low peak power. Moreover, soliton migration through different dispersion regions due to the existence of three ZDWs helps the SC spectrum continue to expand further.

The combination of two factors, the highly nonlinear $Ge_{20}Sb_5Se_{75}$ substrate and the octagonal lattice of the designed structure, helped fibers #F_1, #F_2, and #F_3 demonstrate outstanding advantages in terms of dispersion and nonlinear properties in the wavelength range up to 14 μm. These materials have a flat dispersion profile, low value and very small confinement loss suitable for broadband SC generation applications. **Table 3** compares the dispersion values and characteristic quantities of the proposed PCF with those of other publications on the use of Ge-Sb-Se compounds.

CONCLUSIONS

We designed and modeled forty $Ge_{20}Sb_5Se_{75}$-PCF structures with octagonal lattices. The dispersion and nonlinear properties of the fibers are investigated in detail over a wavelength range of up to 14 μm by numerically solving Maxwell's wave equations using the full-vector finite-difference eigenmode method. Based on the dispersion property and GVD parameter results, we propose three fibers with suitable characteristic quantities for determining the direction of SC generation. Fibers #F_1, #F_2, and #F_3 have very low dispersions——0.88, 0.08, and 1.646 ps/(nm.km)—at pump wavelengths of 2.85, 3.05, and 2.7 μm, respectively; these values are much lower than those of our previous publication[27] on $Ge_{20}Sb_5Se_{75}$-PCF with a hexagonal crystal lattice. In addition, the diversity in the dispersion profiles of the three fibers (all-normal dispersion and anomalous dispersion with one or three ZDWs) strongly influences the characteristics of the SC spectrum. With high nonlinear coefficients of 1010.043, 289.265, and 921.717 $W^{-1}.km^{-1}$ and low confinement losses of 1.305×10^{-5}, 1.549×10^{-11}, and 1.440×10^{-7} dB/m, respectively, three fibers are expected to create SCs with the spectrum broadened further toward the edges. Compared with previous publications, fiber #F_1 has a nonlinear coefficient approximately 1.05 times greater than[10], 2 to 3.5 times greater than[27] and approximately 10 times greater than that of publication[13]. The F3 fiber also has a nonlinear coefficient approximately 4 times greater than[27]. Moreover, the effective mode area is approximately 1.6 times smaller than[10]. Although the nonlinear coefficients of fibers #F_2 and #F_3 are lower than those of fibers[9,10] and[12], they have a much lower confinement loss. These fibers with both all-normal and anomalous dispersion properties are suitable for broadband SC generation in the mid-infrared or infrared region to cover the molecular fingerprint spectral region where distinctive vibrational absorption features are exploited to identify the different molecules. The results of SC based on the #F_1 fiber with a normal dispersion configuration can yield a wide spectrum, high coherence, and low noise. This approach is suitable for applications in the fields of optical coherence tomography and remote sensing[28].

ABBREVIATIONS

SC: Supercontinuum

MIR: Mid-infrared

IR: Infrared

PCFs: Photonic Crystal Fibers

ChG: Chalcogenide

ZDW: Zero dispersion wavelength

GVD: Group Velocity Dispersion

COMPETING INTERESTS

The authors declare that they have no conflicts of interest.

Table 3: Comparison of characteristic quantities with those of other PCF publications using Ge-Sb-Se compounds

#	Material	Λ	d/Λ	Region	λP	D	Lc	γ	A_{eff}
		μm		μm	μm	ps/nm.km	dB/m	$W^{-1}.km^{-1}$	μm^2
$\#F_1$	$Ge_{20}Sb_5Se_{75}$	2.2	0.3	0.5−14	2.85	−0.880	1.305×10^{-05}	1010.043	9.371
$\#F_2$	$Ge_{20}Sb_5Se_{75}$	4.5	0.3	0.5−14	3.05	0.080	1.549×10^{-11}	289.265	30.559
$\#F_3$	$Ge_{20}Sb_5Se_{75}$	2.5	0.3	0.5−14	2.70	1.646	1.440×10^{-07}	921.717	10.837
[9]	$Ge_{15}Sb_{15}Se_{70}$	2.0	0.4	0.5−8.0	3.0	−35	–	1960	approximately 55
[27]	$Ge_{20}Sb_{15}Se_{65}$	1.0	0.23 Λ	3.0−5.0	3.0	500	Approximately 0.01	Approximately 5000	Approximately 2.8
[28]	$Ge_{20}Sb_{15}Se_{65}$	2.6	d=1.2 μm and D = 2.4 μm	2.0−7.0	4.0338	–	a few dB/m	Approximately 1472	Approximately 7.7

AUTHORS' CONTRIBUTIONS

Nguyen Thi Thuy: Methodology, designing and simulating the PCF structures, data processing, plotting the graph, writing the manuscript, answering the reviewer's questions, and providing supervision.

ACKNOWLEDGEMENTS

None

REFERENCES

1. Thuy NT, Duc HT, Lanh CV. Comparison of supercontinuum spectral widths in CCl4-core PCF with square and circular lattices in the claddings. Laser Physics. 2023;33(5):055102-13pp;Available from: https://doi.org/10.1088/1555-6611/acc240.
2. Thuy NT, Lanh CV. Supercontinuum generation based on suspended core fiber infiltrated with butanol. Journal of Optic. 2023;Available from: https://doi.org/10.1007/s12596-023-01323-6.
3. Thuy NT, Lanh CV. Supercontinuum spectra above 2700 nm in circular lattice photonic crystal fiber infiltrated chloroform with the low peak power. Journal of Computational Electronics. 2023;22:1507-1521;Available from: https://doi.org/10.1007/s10825-023-02078-w.
4. Thuy NT, Lanh CV. Broadband supercontinuum generation in hollow-core photonic crystal fibers infiltrated with chloroform. Modern Physics Letters B. 2023;Available from: https://doi.org/10.1142/S0217984923502330.
5. Lanh CV, Thuy NT, Bao TLT, Duc HT, Ngoc VTM, Hieu VL, Van TH. Multioctave supercontinuum generation in As2Se3 chalcogenide photonic crystal fiber. Photonics and Nanostructures - Fundamentals and Applications. 2022;48:100986;Available from: https://doi.org/10.1016/j.photonics.2021.100986.
6. Cheng T, Nagasaka K, Tuan TH, Xue X, Matsumoto M, Tezuka H, Suzuki T, Ohishi Y. Mid-infrared supercontinuum generation spanning 2 to 15.1 μm in a chalcogenide step-index fiber. Optics Letters. 2016;41(9):2117-2120;PMID: 27128088. Available from: https://doi.org/10.1364/OL.41.002117.
7. Eggleton BJ, Luther-Davies B, Richardson K. Chalcogenide photonics. Nature Photonics. 2011;5:141-148;Available from: https://doi.org/10.1038/nphoton.2011.309.
8. Karim MR, Ahmad H, Ghosh S, Rahman BMA. Mid-infrared supercontinuum generation using As2Se3 photonic crystal fiber and the impact of higher-order dispersion parameters on its supercontinuum bandwidth. Optical Fiber Technology. 2018;45:255-266;Available from: https://doi.org/10.1016/j.yofte.2018.07.024.
9. A Medjouri, D Abed. Mid-infrared broadband ultraflat-top supercontinuum generation in dispersion engineered Ge-Sb-Se chalcogenide photonic crystal fiber. Optical Materials. 2019;97:109391;Available from: https://doi.org/10.1016/j.optmat.2019.109391.
10. Medjouri A, Abed D, Becer Z. Numerical investigation of a broadband coherent supercontinuum generation in Ga8Sb32S60 chalcogenide photonic crystal fiber with all-normal dispersion. Opto-Electronics Review. 2019;27(1):1-9;Available from: https://doi.org/10.1016/j.opelre.2019.01.003.
11. Chauhan P, Kumar A, Kalra Y. Mid-infrared broadband supercontinuum generation in a highly nonlinear rectangular core chalcogenide photonic crystal fiber. Optical Fiber Technology. 2018;46:174-178;Available from: https://doi.org/10.1016/j.yofte.2018.10.004.
12. Medjouri A, Abed D. Design and modeling of all-normal dispersion As39Se61 chalcogenide photonic crystal fiber for flat-top coherent mid-infrared supercontinuum generation. Optical Fiber Technology. 2019;50:154-164;Available from: https://doi.org/10.1016/j.yofte.2019.03.021.
13. Chauhan P, Kumar A, Kalra Y. Numerical exploration of coherent supercontinuum generation in multicomponent GeSe2-As2Se3-PbSe chalcogenide based photonic crystal fiber. Optical Fiber Technology. 2020;54:102100;Available from: https://doi.org/10.1016/j.yofte.2019.102100.
14. Chaitanya AGN, Saini TS, Kumar A, Sinha RK. Ultra broadband mid-IR supercontinuum generation in Ge11.5As24Se64.5 based chalcogenide graded-index photonic crystal fiber: design and analysis. Applied Optics. 2016;55(36):10138;PMID: 28059256. Available from: https://doi.org/10.1364/AO.55.010138.
15. Cheng T, Nagasaka K, Tuan TH, Xue X, Matsumoto M, Tezuka H, Suzuki T, Ohishi Y. Mid-infrared supercontinuum generation spanning 2.0 to 15.1μm in a chalcogenide step-index fiber. Optics Letters. 2016;41(9):2117-2120;PMID: 27128088. Available from: https://doi.org/10.1364/OL.41.002117.
16. Wang X, Su J, Wang Y, Yang C, Dai S, Zhang P. High-sensitivity sensing in bare Ge-Sb-Se chalcogenide tapered fiber with optimal structure parameters. Journal of Non-Crystalline Solids. 2021;559:120686;Available from: https://doi.org/10.1016/j.jnoncrysol.2021.120686.
17. Ghosh AN, Meneghetti M, Petersen CR, Bang O, Brilland L, Venck S, Troles J, Dudley JM, Sylvestre T. Chalcogenide-glass polarization-maintaining photonic crystal fiber for mid-infrared supercontinuum generation. Journal of Physics: Photonics. 2019;1(4):044003;Available from: https://doi.org/10.1088/2515-7647/ab3b1e.
18. Wu B, Zhao Z, Wang X, Tian Y, Mi N, Chen P, Xue Z, Liu Z, Zhang P, Shen X, Nie Q, Dai S, Wang R. Mid-infrared supercontinuum generation in a suspended-core tellurium-based chalcogenide fiber. Optical Materials Express. 2018;8(5):1341-1348;Available from: https://doi.org/10.1364/OME.8.001341.
19. Cheng T, Kanou Y, Xue X, Deng D, Matsumoto M, Misumi T, Suzuki T, Ohishi Y. Mid-infrared supercontinuum generation in a novel AsSe2-As2S5 hybrid microstructured optical fiber. Optics Express. 2014;22(19);23019-23025;PMID: 25321772. Available from: https://doi.org/10.1364/OE.22.023019.
20. Kumar CS, Anbazhagan R. Investigation on chalcogenide and silica based photonic crystal fibers with circular and octagonal core. AEU - International Journal of Electronics and Communications. 2017;72:40-45;Available from: https://doi.org/10.1016/j.aeue.2016.11.018.
21. Mi N, Wu B, Jiang L, Sun L, Zhao Z, Wang X, Zhang P, Pan Z, Liu Z, Dai S, Nie Q. Structure design and numerical evaluation of highly nonlinear suspended-core chalcogenide fibers. Journal of Non-Crystalline Solids. 2017;464:44-50;Available from: https://doi.org/10.1016/j.jnoncrysol.2017.03.025.
22. Agrawal GP. Nonlinear fiber optics (5th edition). Elsevier, Amsterdam. ISBN: 978-0-12-397023-7. 2013;Available from: https://doi.org/10.1016/C2011-0-00045-5.
23. Skryabin DV, Luan F, Knight JC, Russell PSJ. Soliton self-frequency shift cancellation in photonic crystal fibers. Science 2003;301(5640):1705-1708;Available from: https://doi.org/10.1126/science.1088516.
24. Dudley JM. Supercontinuum generation in optical fibers, Cambridge University Press. 2010;Available from: https://doi.org/10.1017/CBO9780511750465.
25. Genty G, Lehtonen M, Ludvigsen H. Effect of cross-phase modulation on supercontinuum generated in microstructured fibers with sub30 fs pulses. Optics Express. 2004;12(19):4614-4624;Available from: https://doi.org/10.1364/OPEX.12.004614.
26. Huang Y, Yang H, Zhao S, Mao Y, Chen S. Design of photonic crystal fibers with flat dispersion and three zero dispersion wavelengths for coherent supercontinuum generation in both normal and anomalous regions. The results in Physics. 2021;23:104033;Available from: https://doi.org/10.1016/j.rinp.2021.104033.
27. Vo Thi Minh Ngoc, Tran Viet Thanh, Chu Thi Hoai Sam, Le Tran Bao Tran, Dang Van Trong, Nguyen Thi Thuy, Le Van Hieu, Chu Van Lanh. Optimization of optical properties of Ge20Sb5Se75-based photonic crystal fibers. Vinh University Journal of Sci-

ence, Vol. 51, No. 3A/2022, pp. 12-21;Available from: https://doi.org/10.56824/vujs.2022nt16.
28. A Medjouri, D Abed. Theoretical study of coherent supercontinuum generation in chalcohalide glass photonic crystal fiber. Optik 219; 2020, 165178;Available from: https://doi.org/10.1016/j.ijleo.2020.165178.